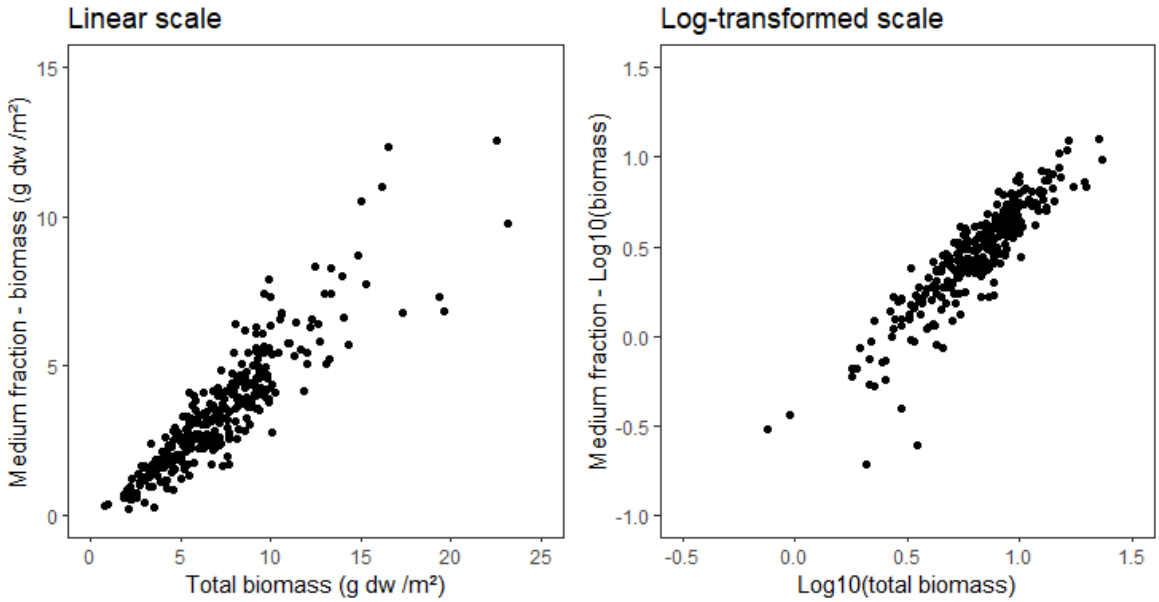

Fig. S1. Scatter plots of zooplankton biomass of the medium fraction versus total biomass for (A) linear (untransformed) and (B) $\log_{10}$ transformed data.

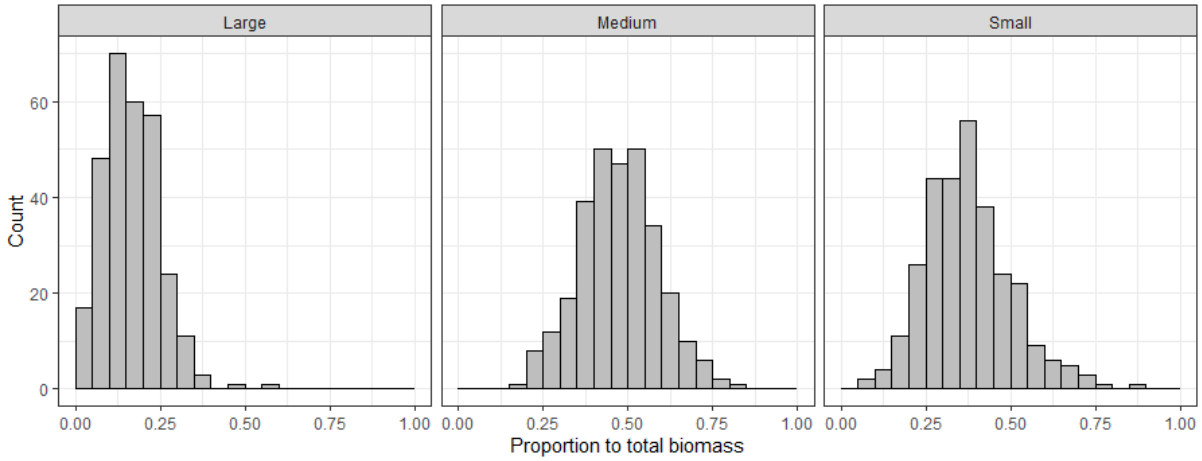

Fig. S2. Frequency distributions of the proportion of biomass of different size fractions to total biomass (large: >2 mm, medium: 1-2 mm, small: <1 mm). The data set excluding the low values was used (based on black points in Fig. 3).

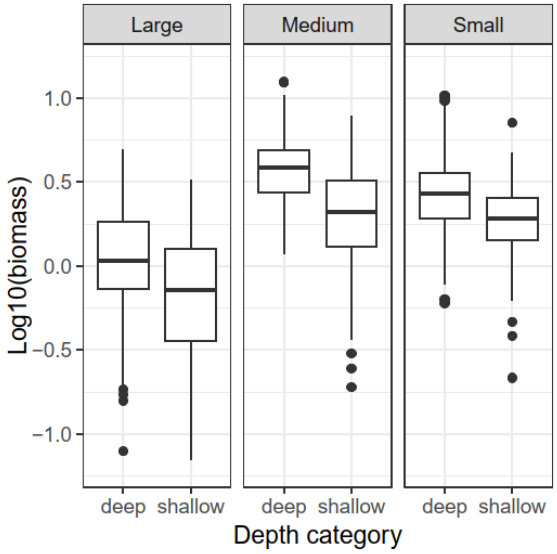

Fig. S3. Box-whisker plots of zooplankton biomass (g DW m^{-2}) of different size fractions (large: >2 mm, medium: 1-2 mm, small: <1 mm) for two different depth categories. The full data set (including the low values, i.e., grey data points in Fig. 3) was used. Shallow: Central Bank, Great Bank, Svalbard South, South East, North East, and Pechora polygons; Deep: Bear Island Trench, Thor Iversen Bank, Hopen Deep, South West, Southeastern Basin, and Svalbard North polygons (see Fig. 1 for polygon locations). The plots show median values (horizontal bar), 25 and 75 percentiles (box), 5 and 95 percentiles (vertical lines), and statistical outliers (points). Data are log_{10}-transformed.

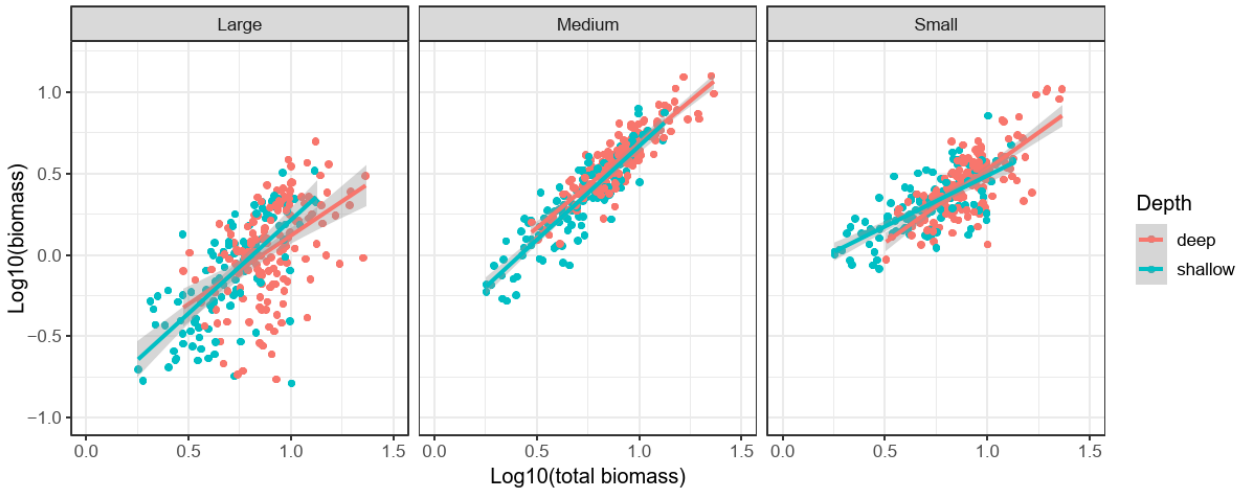

Fig. S4. Linear regressions between zooplankton biomass (g DW m^{-2}) of three size fractions (large: >2 mm, medium: 1-2 mm, small: <1 mm) versus total zooplankton biomass for two different depth categories of deep and shallow polygons. Regression lines with 95 % confidence bands are based on data sets excluding the low values showing scatter (see Fig. 3).

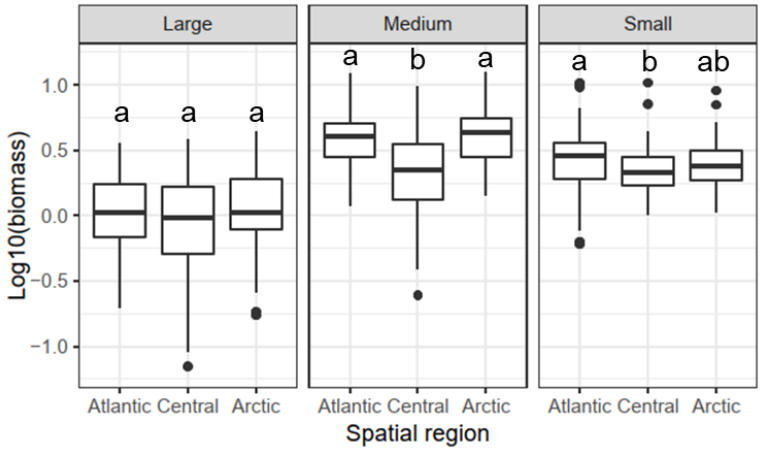

Fig. S5. Zooplankton biomass (g DW m^{-2}) of different size fractions (large: >2 mm, medium: 1-2 mm, small: <1 mm) for three different regions. The full data set (including the low values, i.e., grey data points in Fig. 3) was used. Atlantic = South West, Bear Island Trench, Thor Iversen Bank; Central = Central Bank, Great Bank, Hopen Deep; Arctic = Franz-Victoria Trough, North East, Svalbard North. Different small letters a and b indicate significant differences between regions within a size fraction (Tukey-HSD-post hoc-test, $p<0.05$ following one-way ANOVA).

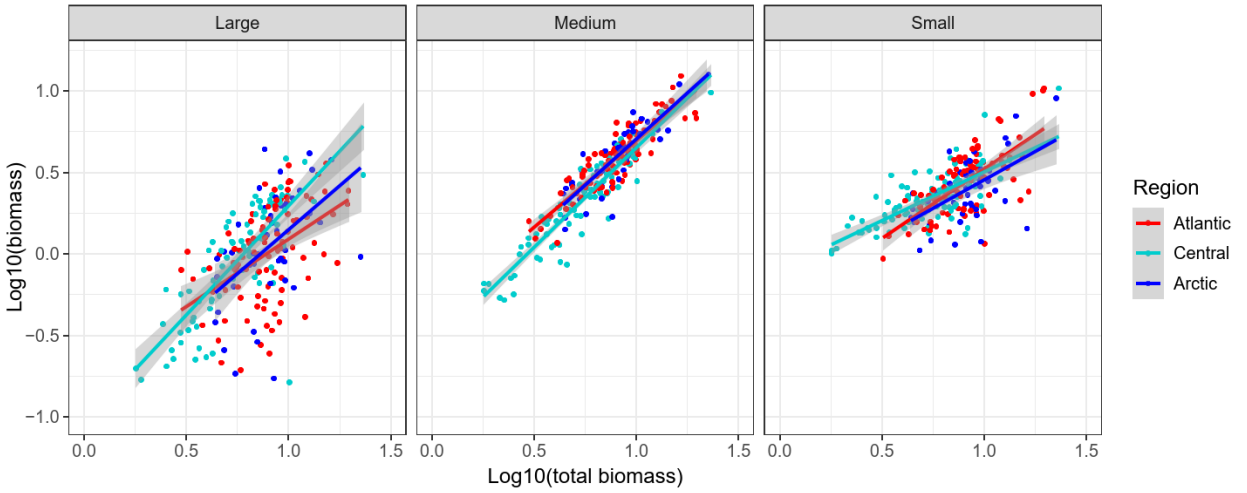

Fig. S6. Linear regressions between zooplankton biomass (g DW m^{-2}) of three size fractions (large: >2 mm, medium: 1-2 mm, small: <1 mm) and total zooplankton biomass for three different regions (see legend to Fig. S5). Regression lines with 95 % confidence bands are based on data sets excluding the low values showing scatter in Fig. 3.

Fig. S7. Zooplankton biomass (g DW m^{-2}) of different size fractions (large: >2 mm, medium: 1-2 mm, small: <1 mm) for two different time periods (older: 1989-2006, recent: 2007-2020). The full data set (including the low values, i.e., both black and grey data points in Fig. 3) was used. Data are log_{10}-transformed.

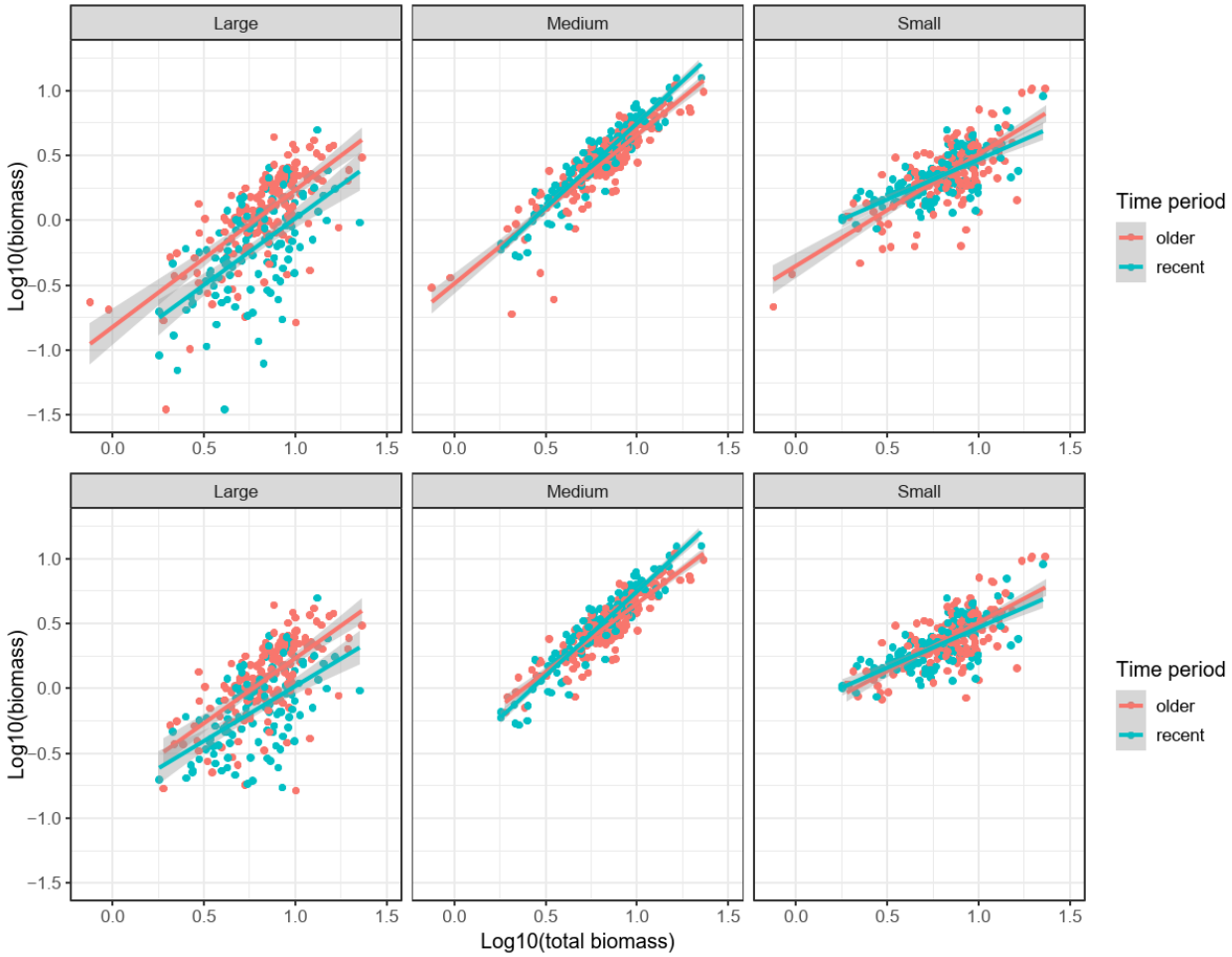

Fig. S8. Linear regressions between zooplankton biomass (g DW m^{-2}) of three size fractions (large: >2 mm, medium: 1-2 mm, small: <1 mm) and total zooplankton biomass for two different time periods (older: 1989-2006, recent: 2007-2020). Regression lines with 95 % confidence bands are based on the full data sets (upper panels) and on data sets excluding the low values showing scatter (lower panels). Data are log_{10}-transformed.

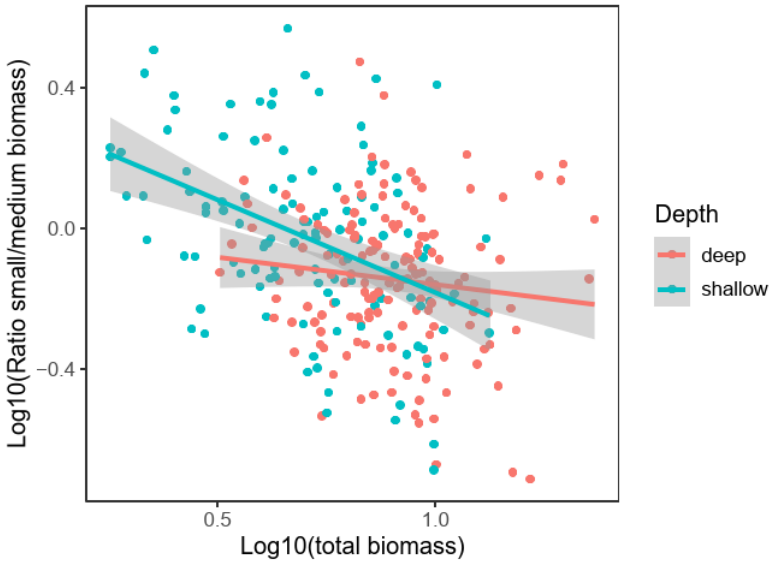

Fig. S9. Scatter plots and regression lines with 95 % confidence bands for relationships between biomass ratio of the small to medium size fraction and total zooplankton biomass for two different depth categories. The restricted data set was used (based on black data points in Fig. 3); data are $\log_{10}$ transformed.

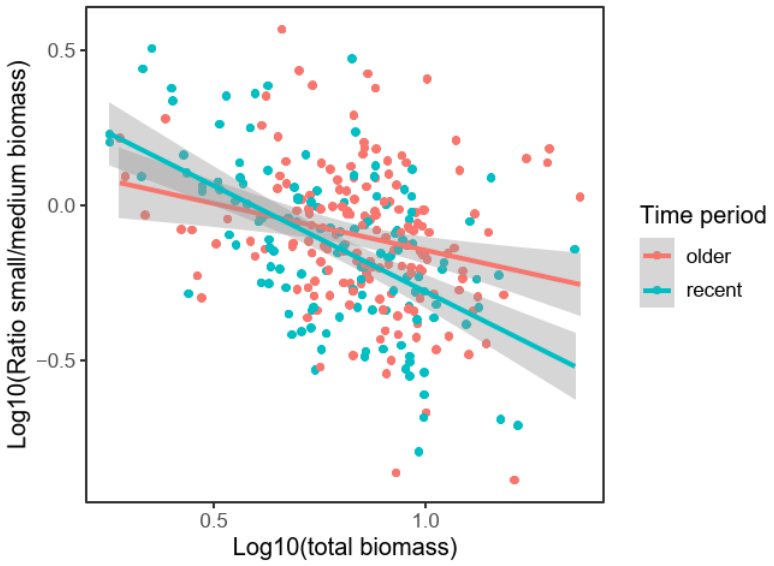

Fig. S10. Scatter plots and regression lines with 95 % confidence bands for relationships between biomass ratio of the small to medium size fraction and total zooplankton biomass for two different time periods (older: 1989-2006, recent: 2007-2020). The restricted data set was used (based on black data points in Fig. 3); data are $\log_{10}$ transformed.